

# Adenosine A<sub>1</sub>-Receptor Modulation of Glutamate-Induced Calcium Influx in Rat Retinal Ganglion Cells

Andrew T. E. Hartwick,<sup>1,2</sup> Mélanie R. Lalonde,<sup>1,3</sup> Steven Barnes,<sup>1,3,4</sup> and William H. Baldrige<sup>1,2,4</sup>

**PURPOSE.** Although adenosine receptors (A<sub>1</sub>-Rs and A<sub>2</sub>-Rs) have been identified in the mammalian retina, the role of adenosine in this tissue is not fully understood. The purpose of this work was to investigate the action of adenosine on glutamate-induced calcium influx in rat retinal ganglion cells (RGCs) and to determine whether adenosine modulates RGC voltage-gated calcium channels.

**METHODS.** Purified RGC cultures were generated from neonatal rats with a two-step panning procedure. Isolated RGCs were loaded with the ratiometric calcium-indicator dye fura-2, and the effect of adenosine (and related agonists and antagonists) on intracellular calcium levels ( $[Ca^{2+}]_i$ ) during exposure to glutamate (10  $\mu$ M with 10  $\mu$ M glycine) was assessed. The effect of adenosine on calcium channel currents was also studied in isolated RGCs with whole-cell patch-clamp techniques. In addition, the effect of adenosine on  $[Ca^{2+}]_i$  was investigated in fura dextran-loaded RGCs in an intact adult rat retina preparation.

**RESULTS.** In isolated RGCs, adenosine (10 and 100  $\mu$ M) significantly reduced the glutamate-induced increase in  $[Ca^{2+}]_i$  (~30%). The effect of adenosine was blocked by the A<sub>1</sub>-R antagonist 8-cyclopentyl-1,3-dipropylxanthine (DPCPX), but not by the A<sub>2</sub>-R antagonist 3,7-dimethyl-1-propargylxanthine (DMPX). Adenosine (10  $\mu$ M) inhibited calcium channel currents by 43%, and again this effect was blocked by DPCPX, but not DMPX. Adenosine (100  $\mu$ M) also significantly reduced the elevation of  $[Ca^{2+}]_i$  in RGCs in the intact retina during exposure to *N*-methyl-D-aspartate (NMDA; 100  $\mu$ M).

**CONCLUSIONS.** Adenosine can inhibit glutamate-induced calcium influx and voltage-gated calcium currents in rat RGCs through A<sub>1</sub>-R activation. This work supports a role for adenosine as a neuromodulator of mammalian RGCs. (*Invest Ophthalmol Vis Sci.* 2004;45:3740–3748) DOI:10.1167/iovs.04-0214

Adenosine is now recognized as an important neuromodulator in the central nervous system (CNS).<sup>1</sup> Under normal physiological conditions, the majority of extracellular adeno-

sine is thought to be generated by the conversion of the neurotransmitter adenosine 5'-triphosphate (ATP) by ectonucleotidases.<sup>2</sup> In the retina, the release of ATP from cholinergic amacrine<sup>3</sup> and Müller<sup>4</sup> cells represents potential sources of adenosine in the inner retina.

Four adenosine receptors have been cloned and characterized, all of which are coupled to G-proteins and are designated as A<sub>1</sub>, A<sub>2A</sub>, A<sub>2B</sub>, and A<sub>3</sub>.<sup>5</sup> Whereas A<sub>3</sub> adenosine receptors have not yet been identified in the retina, A<sub>1</sub> and A<sub>2</sub> receptors (A<sub>1</sub>-Rs and A<sub>2</sub>-Rs) have been found in the retinas of several vertebrates and appear to have distinct areas of distribution: A<sub>1</sub>-Rs predominantly in the inner retina, and A<sub>2</sub>-Rs in the outer retina.<sup>6</sup> In the rat retina, autoradiographic receptor binding<sup>7</sup> and in situ hybridization<sup>8</sup> studies have provided evidence for the presence of A<sub>1</sub>-Rs in the inner plexiform (IPL) and ganglion cell (GCL) layers.

The presence of A<sub>1</sub>-Rs in the IPL and GCL suggests that adenosine may influence retinal ganglion cells (RGCs). Throughout the CNS, A<sub>1</sub>-R activation generally results in presynaptic inhibition through modulation of potassium and calcium currents.<sup>1,5</sup> Recently, adenosine has been shown to decrease voltage-gated calcium channel (VGCC) currents in goldfish<sup>9,10</sup> and salamander<sup>11</sup> RGCs through A<sub>1</sub>-R activation. It is not known if adenosine also modulates calcium currents in mammalian RGCs. Although the modulation of RGC calcium channels by adenosine may be relevant to presynaptic inhibition of glutamate release from RGC terminals in the brain,<sup>9,10,12</sup> it is also possible that adenosine acts within the retina to modulate postsynaptically the effect of glutamate, released from bipolar cells, on RGC activity. In this work, adenosine decreased glutamate receptor-induced calcium influx in rat RGCs in both purified RGC cultures and an intact retina preparation. Adenosine also modulated calcium channel currents in isolated rat RGCs. The pharmacology of the effects of adenosine on glutamate-induced calcium influx and calcium currents was, in each case, consistent with an action at A<sub>1</sub>-Rs.

## METHODS

### Materials

The Neurobasal-A culture medium, B27 supplements, Dulbecco's phosphate-buffered saline (DPBS), glutamine, and trypsin were obtained from Invitrogen-Gibco (Burlington, Ontario, Canada). The papain and DNase were from Worthington Biochemicals (Lakewood, NJ). Rhodamine B dextran, fura dextran, fura-2 acetoxymethyl (AM) ester and pluronic acid F-127 were purchased from Molecular Probes (Eugene, OR). Regeneron (Tarrytown, NY) generously provided brain-derived neurotrophic factor (BDNF) and ciliary neurotrophic factor (CNTF; axokine protein). Unless noted otherwise, all other chemicals and reagents were obtained from Sigma-Aldrich (Oakville, Ontario, Canada).

Stock solutions of L-glutamate, glycine, *N*-methyl-D-aspartate (NMDA), and adenosine were prepared before each experiment and were dissolved in the experimental Hanks' balanced salt solution (HBSS). *N*<sup>6</sup>-cyclohexyladenosine (CHA) and 5'-(*N*-cyclopropyl) carboxamidoadenosine (CPA) were first dissolved as a stock solution (10 mM) in 0.1 N HCl. 8-Cyclopentyl-1,3-dipropylxanthine (DPCPX) was

From the <sup>1</sup>Retina and Optic Nerve Research Laboratory and the Departments of <sup>2</sup>Anatomy and Neurobiology, <sup>3</sup>Physiology and Biophysics, and <sup>4</sup>Ophthalmology and Visual Sciences, Dalhousie University, Halifax, Nova Scotia, Canada.

Supported by Canadian Institute of Health Research (CIHR) operating Grants MOP-15683 (WHB) and MT-10868 (SB); a pilot project grant from the Canadian Optometric Education Trust Fund; an E. A. Baker Fellowship (ATEH) and Scholarship (MRL) cosponsored by CIHR and the Canadian National Institute for the Blind; and a TLC Laser Eye Center-sponsored Ezell Fellowship from the American Optometric Foundation (ATEH).

Submitted for publication February 26, 2004; revised May 26, 2004; accepted June 7, 2004.

Disclosure: A.T.E. Hartwick, None; M.R. Lalonde, None; S. Barnes, None; W.H. Baldrige, None

The publication costs of this article were defrayed in part by page charge payment. This article must therefore be marked "advertisement" in accordance with 18 U.S.C. §1734 solely to indicate this fact.

Corresponding author: William H. Baldrige, Dalhousie University, Halifax, Nova Scotia B3H 4H7, Canada; wbaldrid@dal.ca.

first dissolved in dimethyl sulfoxide (DMSO), and 3,7-dimethyl-1-propargylxanthine (DMPX) was first dissolved in purified water (10 mM stock for both). Aliquots of CHA, CPCA, DPCPX, and DMPX stock solutions were stored at  $-30^{\circ}\text{C}$  before use.

### Purified RGC Culture

All procedures were performed in accordance with the ARVO Statement for the Use of Animals in Ophthalmic and Vision Research and the Dalhousie University Committee for the Use of Laboratory Animals. Natural litters (1–10 pups for each experiment) of Long-Evans rats (Charles River, Montreal, Quebec, Canada) were killed at postnatal day (P)7 to P8 by overexposure to halothane and decapitation. After the eyes were enucleated, the anterior segment and lens were removed, and the posterior eyecups were immersed in dissection medium consisting of Hibernate-A medium (BrainBits, Springfield, IL)<sup>13</sup> with 2% B27 supplements and 10  $\mu\text{g}/\text{mL}$  gentamicin. The retinas were dissected and maintained in the dissection medium until all retinas were isolated.

The retinal tissue was incubated for 30 minutes at  $37^{\circ}\text{C}$  in a papain solution (165 U in 10 mL DPBS) containing 1 mM L-cysteine and 0.004% DNase. The papain-treated retinas were then triturated sequentially in DPBS containing 1.5 mg/mL ovomucoid (Roche Diagnostics, Laval, Quebec, Canada), 1.5 mg/mL bovine serum albumin (BSA), and 0.004% DNase. In addition, this solution contained the rabbit anti-rat macrophage antibodies (1:75; Axell Brand; Accurate Chemical, Westbury, NY) required for the macrophage panning step. The suspension was centrifuged, rewashed in a high concentration ovomucoid/BSA solution (10 mg/mL each in DPBS), and the dissociated cells were resuspended in DPBS with 0.2 mg/mL BSA and 5  $\mu\text{g}/\text{mL}$  insulin.

Purified RGC cultures were generated using a two-step panning (antibody-mediated plate adhesion) procedure, as described previously.<sup>14,15</sup> Briefly, the mixed retinal cell suspension was incubated on Petri dishes coated with affinity-purified goat anti-rabbit IgG (H+L) antibodies (Jackson ImmunoResearch, West Grove, PA) to remove macrophages from the suspension. The remaining cells were then transferred to a Petri dish that had first been coated with affinity-purified goat anti-mouse IgM ( $\mu$  chain) antibodies (Jackson ImmunoResearch) and second with anti-Thy-1.1 monoclonal IgM antibodies (cell line T11D7e2; TIB-103; American Type Culture Collection, Manassas, VA). After 30 minutes, the dish was repeatedly rinsed with DPBS to remove any nonadherent cells, and the remaining adherent cells (RGCs) were released by first incubating the cells in a 0.125% trypsin solution and then manually pipetting an enzyme inhibitor solution (30% FBS in Neurobasal-A) along the surface of the dish.

The RGCs were plated onto poly-D-lysine/laminin-coated glass coverslips (12 mm round, Biocoat; BD Biosciences, Bedford, MA) in 24-well tissue culture plates at a density of  $1.5 \times 10^4$  cells per well. The cells were cultured in 600  $\mu\text{L}$  of serum-free culture medium consisting of Neurobasal-A with 2% B27 supplements, 1 mM glutamine, 50 ng/mL BDNF, 10 ng/mL CNTF, 5  $\mu\text{M}$  forskolin, and 10  $\mu\text{g}/\text{mL}$  gentamicin.<sup>15,16</sup> Cultures were maintained at  $37^{\circ}\text{C}$  in a humidified 5%  $\text{CO}_2$ -95% air atmosphere. All experiments on the isolated RGCs were performed on the 2 days after the day of cell dissociation and panning.

### Retrograde Labeling of RGCs

To confirm the purity and yield of RGCs obtained with the panning procedure, preliminary studies were performed using a retrograde label to identify the RGCs in culture ( $n = 3$  separate panning experiments). RGCs can be distinguished from other retinal cells through the use of a fluorescent retrograde label injected into the superior colliculus, the primary projection site for RGCs in rats. The rats (aged P6) were put under halothane anesthesia, and a longitudinal incision was made along the midline of the scalp to expose the skull. Two injections each of 2  $\mu\text{L}$  rhodamine B dextran (10,000 MW, 10% solution dissolved in water) were made through the skull on each side of the brain with a 10- $\mu\text{L}$  syringe (Hamilton, Reno, NV) fitted with a 26-gauge needle. The injections were performed at a depth of 4 mm and at a position 2 mm lateral to the sagittal sinus, just rostral to its intersection with the

transverse sinus.<sup>14,17</sup> To allow for retrograde transport, the RGC cultures were generated from these rats 2 days after the rhodamine dextran injection. The rhodamine dextran was detected in the cultured RGCs with a rhodamine filter set (XF101-2, excitation 525 nm; emission 565 nm; dichroic 560 nm; Omega Optical, Brattleboro, VT) fitted to the microscope rig described later.

### Calcium Imaging of Isolated RGCs

The RGCs were loaded with the ratiometric calcium-indicator dye fura-2. Cells were incubated in 5  $\mu\text{M}$  fura-2 AM dissolved in modified  $\text{Mg}^{2+}$ -free HBSS (2.6 mM  $\text{CaCl}_2$ , 15 mM HEPES [pH 7.4]) for 30 minutes in the dark at  $37^{\circ}\text{C}$ . The fura-2 AM was first dissolved in DMSO (0.1% final concentration in HBSS) and then solubilized in HBSS containing 0.1% pluronic acid F-127.

Coverslips containing the fura-2-loaded RGCs were then transferred to a microscope chamber ( $\Delta\text{TC3}$ ; Biopatch, Butler, PA) that was constantly superfused with the  $\text{Mg}^{2+}$ -free HBSS at  $34^{\circ}\text{C}$  to  $36^{\circ}\text{C}$  (SH-27 Inline heater, TC-324B controller; Warner Instruments, Hamden, CT) and bubbled with 100% oxygen. A 75-W xenon lamp (LUDL Electronic Products, Hawthorne, NY) and the appropriate filters (XF04 set, excitation 340 or 380 nm; emission 510 nm; dichroic  $>430$  nm; Omega Optical) were used to generate fura-2 fluorescence. Alternation of the excitation wavelength from 340 to 380 nm was controlled by an optical filter changer (Lambda 10-2; Sutter Instruments, Novato, CA) with an electronic shutter (Uniblitz, Rochester, NY), to limit each period of illumination to 400 ms. To reduce photodamage and photobleaching, excitation illumination was filtered with a  $-0.5$ -log neutral-density filter and  $320 \times 256$ -pixel ( $4 \times 4$ -binned) images were acquired. Fluorescence images were captured (8-bit) with a cooled charged-coupled device (CCD) camera (Sensicam; PCO Computer Optic, Kelheim, Germany) fitted to a microscope (Axioskop FS; Carl Zeiss Meditec, Oberkochen, Germany) using a water-immersion objective (NA 0.80 W; Achroplan 40 $\times$ ; Carl Zeiss Meditec). The images of RGC fluorescence at 340 and 380-nm excitation were converted to ratiometric (340 nm/380 nm) images by an imaging system (Imaging Workbench 2.2; Axon Instruments, Foster City, CA) and saved to the hard disc of a computer. The background fluorescence was measured from a region on the coverslip devoid of RGCs and subtracted from each image. The mean fura-2 ratio for each RGC was calculated over a large area of the RGC soma, well separated from the edge of the cell.

All treatment solutions were dissolved in the  $\text{Mg}^{2+}$ -free HBSS and delivered to the chamber by a peristaltic pump (Gilson, Middleton, WI) at a rate of approximately 1 mL/min. The intracellular free calcium concentration ( $[\text{Ca}^{2+}]_i$ ) was elevated in the isolated RGCs by application of a short pulse (30 seconds) of 10  $\mu\text{M}$  glutamate plus 10  $\mu\text{M}$  glycine, a coagonist of glutamate at the NMDA-type glutamate receptor.<sup>18</sup> During treatments, image pairs were collected as often as every 3 seconds, but to limit photodamage, images were collected less frequently (20 seconds) during intervening periods. The time between consecutive glutamate exposures was kept at 15 minutes to allow sufficient time for  $[\text{Ca}^{2+}]_i$  to return to a baseline level.

Fura-2 ratios ( $R$ ) were converted to  $[\text{Ca}^{2+}]_i$  in separate calibration experiments using the formula<sup>19,20</sup>

$$[\text{Ca}^{2+}]_i = [K_d(F_o/F_s)] \left[ (R - R_{\min}) / (R_{\max} - R) \right],$$

with a  $K_d$  for fura-2 of 224 nM, and where  $F_o/F_s$  is the ratio of fluorescence intensity at 380 nm excitation in calcium-free solution over the intensity in solution with saturated calcium levels. Superfusion of the isolated RGCs with calcium-free HBSS (10 mM  $\text{Mg}^{2+}$ , 2 mM BAPTA [bis-(*o*-aminophenoxy)-*N,N,N'*-tetraacetic acid], and 10  $\mu\text{M}$  ionomycin) was used to determine the minimum value for the fura-2 ratio ( $R_{\min}$ ), after which the cells were superfused with a saturated calcium solution (0.9% saline with 20 mM  $\text{Ca}^{2+}$ , 10  $\mu\text{M}$  ionomycin) to determine the maximum fura-2 ratio ( $R_{\max}$ ). Mean values for  $F_o/F_s$ ,  $R_{\min}$ , and  $R_{\max}$  were calculated from 5 to 10 RGCs and the calibration procedure was repeated every 3 weeks. Conversion of the fura-2 ratios to  $[\text{Ca}^{2+}]_i$  allowed an approximation of absolute calcium levels, but as

all comparisons of the effect of adenosine and related drugs were within-cell comparisons, the conversion to  $[Ca^{2+}]_i$  did not alter the presence or absence of a given effect or its statistical significance.

Calcium influx was measured as the peak  $[Ca^{2+}]_i$  after each glutamate exposure minus the average baseline  $[Ca^{2+}]_i$  measured before the first glutamate exposure. RGCs that had a negligible response to glutamate (peak  $[Ca^{2+}]_i < 150$  nM) were excluded from the analysis.

### Electrophysiological Recordings from Isolated RGCs

Whole-cell patch-clamp recordings of calcium channel currents, using barium as a charge carrier, were obtained from individual RGCs in the purified culture that were selected for patching with a microscope (Diaphot; Nikon, Melville, NY). The standard bath solution contained (in mM): 115 NaCl, 2.5 KCl, 5 CsCl, 10 BaCl<sub>2</sub>, 15 tetraethylammonium-Cl (TEACl), 10 glucose, and 15 HEPES, adjusted to pH 7.6 with NaOH, and the intracellular pipette solution contained (in mM): 140 CsCl, 0.8 MgCl<sub>2</sub>, 0.1 CaCl<sub>2</sub>, 1:4 EGTA:CsOH, 10 HEPES, 1 Mg<sup>2+</sup>-ATP, and 0.2 Na<sup>+</sup>-guanosine triphosphate (GTP), adjusted to pH 7.2 with CsOH. Tetrodotoxin (TTX; 1 μM) was added to the bath solution to eliminate any contribution from sodium channels to the whole-cell current. Solutions were applied at room temperature (21–25°C) through a gravity-driven perfusion system through an eight-way valve at approximately 2 mL/min.

Calcium channel currents were recorded from RGCs using the ruptured-patch technique. Patch electrodes were pulled from fire-polished microhematocrit capillary tubes (VWR Scientific, West Chester, PA) using a two-step vertical pipette puller (model 730; David Kopf Instruments, Tujunga, CA). Pipette tips were first dipped in standard intracellular solutions and then back-filled with the same solution. Filled pipettes had 5- to 10-MΩ tip resistances, measured in the standard bath. The bath reference electrode consisted of a bath solution-filled agar bridge with an AgCl wire (World Precision Instruments, Sarasota, FL). Offset currents were nulled before seals were made. Whole-cell voltage was clamped with an amplifier (Axopatch-1D; Axon Instruments), using whole-cell capacitance and series resistance compensation to reduce capacitive artifacts. The current signal was filtered at 1 to 3 kHz (4302 Dual 24dB/octave filter; Ithaco, Ithaca, NY) and digitized at 1 kHz with an interface (Indec Systems, Sunnyvale, CA) for storage on the hard disc of a computer running signal-acquisition software (Basic-Fastlab; Indec Systems). The software generated the voltage-clamp commands and provided some data analysis.

Holding potential was set at –60 mV and voltage steps consisted of 10-mV increments of 100-ms duration from –70 mV to +40 mV every 1 second. Current-voltage (I-V) relations were measured by calculating the mean current ~10 ms before the end of each voltage step. Several successive points were averaged together in some records where currents changed slowly in time, to reduce storage requirements. For illustration, one to three points at the peak of each capacitance current transient have been removed from some records.

### Calcium Imaging of RGCs in Retinal Wholemounts

Calcium-imaging experiments on RGCs in an intact rat retina preparation were performed with a method that was previously developed for use on rabbit retinas.<sup>21</sup> Adult Long-Evans rats (>10 weeks old) were killed by pentobarbital overdose and both eyes enucleated. The anterior segment and vitreous were removed, and the posterior segment was immersed in the modified Mg<sup>2+</sup>-free HBSS (2.6 mM CaCl<sub>2</sub>, 15 mM HEPES [pH 7.4]) that was bubbled continuously with 100% oxygen. The underlying sclera was pinned to a silicone-lined (Sylgard; Dow Corning, Midland, MI), glass Petri dish, and the retina was dissected from the eyecup by slowly peeling the sclera away from the retina with a flat spatula. The retina was floated onto a glass microscope slide, and the peripheral retinal edges were trimmed with a scalpel blade. The retina was then mounted on black filters (HABP 045; Millipore, Bedford, MA) with the RGC layer uppermost.

A small amount (~0.5 μL) of 10,000 MW dextran-conjugated fura calcium-indicator dye (10% wt/vol; dissolved in purified water) was ejected to the tip of a tapered 26-gauge needle fitted to a 10-μL syringe (Hamilton, Reno, NV), and the needle tip was then inserted into the flatmounted retina, passing through all the retinal layers. As described previously,<sup>21</sup> the dextran-conjugated dye labels a variety of neuronal cell types near the injection site, but it also labels RGC axons that pass through the injection site. The retinas were then incubated at room temperature in HBSS bubbled continuously with 100% oxygen for 3 to 5 hours before calcium imaging, to allow for the retrograde transport of the fura dextran to RGC somata.

The NMDA-induced calcium influx was measured as the peak fura ratio minus the baseline fura ratio (the average ratio measured in the five images before each NMDA exposure) in the RGC somata. The time between consecutive NMDA exposures was 20 to 25 minutes.

### Data Analysis

All data are expressed as the mean ± SEM. For all calcium-imaging experiments, the calcium influx was normalized to the initial glutamate (isolated cells) or NMDA (intact retina) treatment. Statistical within-cell comparisons of the effect of adenosine and/or related drugs were made on the normalized data using the nonparametric Friedman repeated-measures ANOVA and Student-Newman-Keuls (SNK) multiple-comparison post hoc test. For the electrophysiology experiments, comparisons of the current before and after treatment with drug(s) were made on the normalized data with the Mann-Whitney test. Statistical analysis was performed on computer (SigmaStat software; SPSS Science, Chicago IL).

## RESULTS

### Effect of Adenosine on Glutamate-Induced Calcium Influx in RGCs in Purified Cultures

In immunopanned cultures generated from rats that had the rhodamine dextran injection in the superior colliculus, more than 97% of the plated cells exhibited positive rhodamine fluorescence, thereby confirming their identity as RGCs (Figs. 1A–D). The few cells not labeled were generally smaller and easy to distinguish morphologically from the identified RGCs (Figs. 1C, 1D) and cells of this type were not used in subsequent imaging or patch-clamp experiments. The yield ranged from 15,000 to 30,000 RGCs per retina. Calcium-imaging experiments were performed on the isolated RGCs after 1 to 2 days of culture, and the ratio of fura-2 fluorescence (340 nm/380 nm, converted to  $[Ca^{2+}]_i$  after calibration experiments<sup>19,20</sup>) was measured in the somata of individual RGCs (Figs. 1E–G). The protocol of a 30-second exposure to 10 μM glutamate plus 10 μM glycine (hereafter referred to as glutamate, with the addition of glycine implied) was chosen because it resulted in reproducible increases in  $[Ca^{2+}]_i$  within the dynamic range (below saturation) of fura-2 fluorescence.

To test the effect of adenosine, we exposed each RGC to 10 μM glutamate four consecutive times, with the second and fourth treatments occurring with adenosine present (Fig. 2A). In the presence of 10 μM adenosine, calcium influx was significantly reduced (mean influx, 68.7% ± 7.1% and 68.2% ± 6.6% of the initial response; *n* = 15; *P* < 0.01) compared with the two responses in the absence of adenosine (Fig. 2B). Increasing the concentration of adenosine from 10 to 100 μM resulted in a similar reduction (70.1% ± 3.8% and 62.0% ± 4.5% of the initial response; *n* = 15; *P* < 0.01) of the glutamate-induced calcium influx (Fig. 2B). This suggests that the maximum effect of adenosine is achieved at 10 μM in isolated RGCs.

### Pharmacology of the Effect of Adenosine on Glutamate-Induced Calcium Influx

To determine whether the inhibitory effect of adenosine on glutamate-induced calcium influx was mediated by either

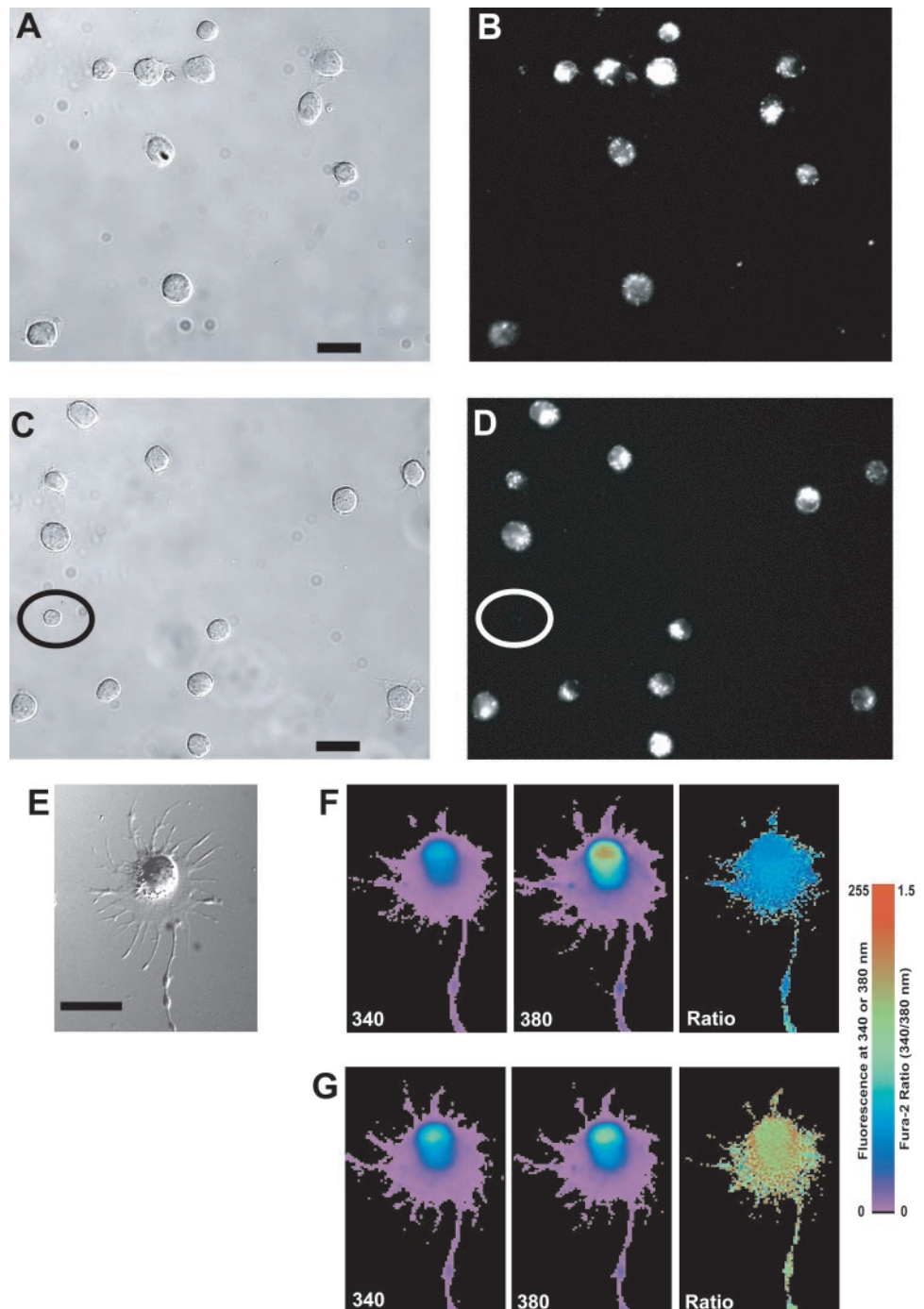


**FIGURE 1.** Glutamate increased  $[Ca^{2+}]_i$  in rat RGCs in a purified culture. (A, C) Differential interference contrast (DIC) images of cultured cells 6 hours after plating and (B, D) fluorescence micrographs of the same cells, to identify RGCs retrogradely labeled with rhodamine dextran. The panning method generated RGC cultures more than 97% pure (lone cell not exhibiting rhodamine dextran fluorescence is encircled). (E) DIC image of an RGC 1 day after dissociation and (F) the pseudocolor representation of its fluorescence at 340 and 380 nm excitation (510 nm emission) and the resultant fura-2 ratio (340/380 nm) at baseline and (G) at peak response to 10  $\mu$ M glutamate plus 10  $\mu$ M glycine. Scale bar, 25  $\mu$ m.

$A_1$ -Rs or  $A_2$ -Rs, additional calcium-imaging experiments were performed on the cultured RGCs, with the appropriate adenosine receptor antagonists and agonists. Individual RGCs were again exposed to four consecutive treatments of 10  $\mu$ M glutamate. Adenosine was present during the second exposure, and adenosine and either the  $A_1$ -R antagonist DPCPX (Fig. 3A) or the  $A_2$ -R antagonist DMPX (Fig. 3B) were present during the third exposure. Adenosine alone significantly decreased ( $P < 0.01$ ) the glutamate-induced calcium influx in both groups, consistent with the results shown in Figure 2, and the effect of adenosine was almost completely blocked by DPCPX but not DMPX. In the presence of both adenosine and DPCPX, the glutamate-induced calcium influx ( $92.1\% \pm 8.2\%$  of initial response;  $n = 14$ ) was not significantly different ( $P > 0.05$ ) from either the initial or the

recovery response to glutamate (Fig. 3C). In contrast, in the presence of both adenosine and DMPX, the calcium influx ( $61.2\% \pm 5.1\%$  of initial response;  $n = 14$ ) remained significantly reduced ( $P < 0.01$ ) compared with the responses to glutamate alone (Fig. 3C).

In experiments using adenosine agonists, the presence of either 1 or 10  $\mu$ M of the  $A_1$ -R agonist CHA resulted in a significant decrease ( $P < 0.01$ ) in the glutamate-induced calcium influx (to  $76.4\% \pm 7.9\%$  and  $64.3\% \pm 5.9\%$  of the initial response, respectively;  $n = 15$  for both; Figs. 3D, 3E). This decrease was similar in magnitude to that observed with adenosine (Fig. 2). At 1  $\mu$ M, the  $A_2$ -R agonist CPCA did not affect ( $P = 0.25$ ) the glutamate-induced calcium influx (influx  $96.0\% \pm 7.7\%$  of the initial response;  $n = 15$ ). At 10  $\mu$ M, CPCA had a small (influx  $85.4\% \pm 3.6\%$  of initial response;  $n = 15$ ) but

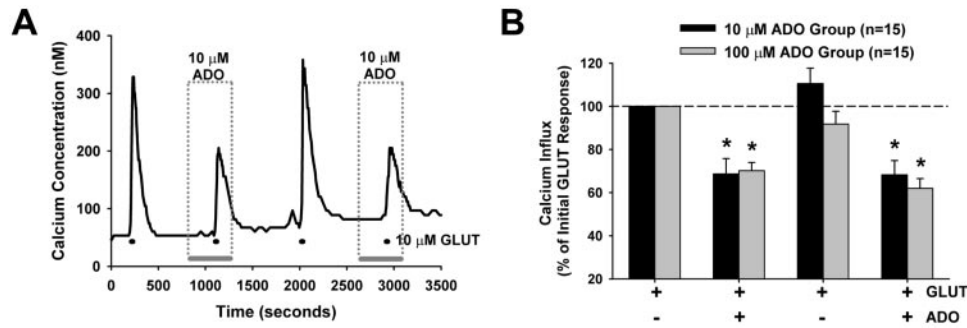


**FIGURE 2.** Adenosine (ADO) inhibited glutamate-induced calcium influx in isolated RGCs. (A)  $[Ca^{2+}]_i$  trace from a cultured RGC illustrating the effect of 10  $\mu$ M adenosine on the RGC response to 10  $\mu$ M glutamate (GLUT; with 10  $\mu$ M glycine). Cells were exposed to glutamate four times with adenosine present during the second and fourth treatments. (B) Mean data for all RGCs in studies using 10 and 100  $\mu$ M adenosine, normalized to initial glutamate response (dashed line, 100%). \* $P < 0.01$  compared with both control glutamate responses (Friedman ANOVA, SNK).

significant ( $P < 0.01$ ) effect (Fig. 3E). The recovery responses to glutamate in each of the four agonist treatment groups were not significantly different ( $P > 0.05$ ; data not shown) from the initial response, indicating that agonist effects were not due to “run-down.” The full recovery of the glutamate response after washing (also see recovery responses in Figs. 2B and 3C) indicates that the inhibitory effect of adenosine on glutamate-induced calcium influx in isolated rat RGCs is reversible.

### Effect of Adenosine on Calcium Channel Currents in Isolated RGCs

In the electrophysiology experiments, adenosine significantly inhibited ( $P < 0.01$ ) calcium channel current (mean inhibition,  $43.2\% \pm 5.9\%$ ;  $n = 7$ ) in the isolated RGCs (Figs. 4A, 4G), and there was no apparent voltage dependence of the inhibitory effect as seen in the current-voltage relationship (Fig. 4B). In

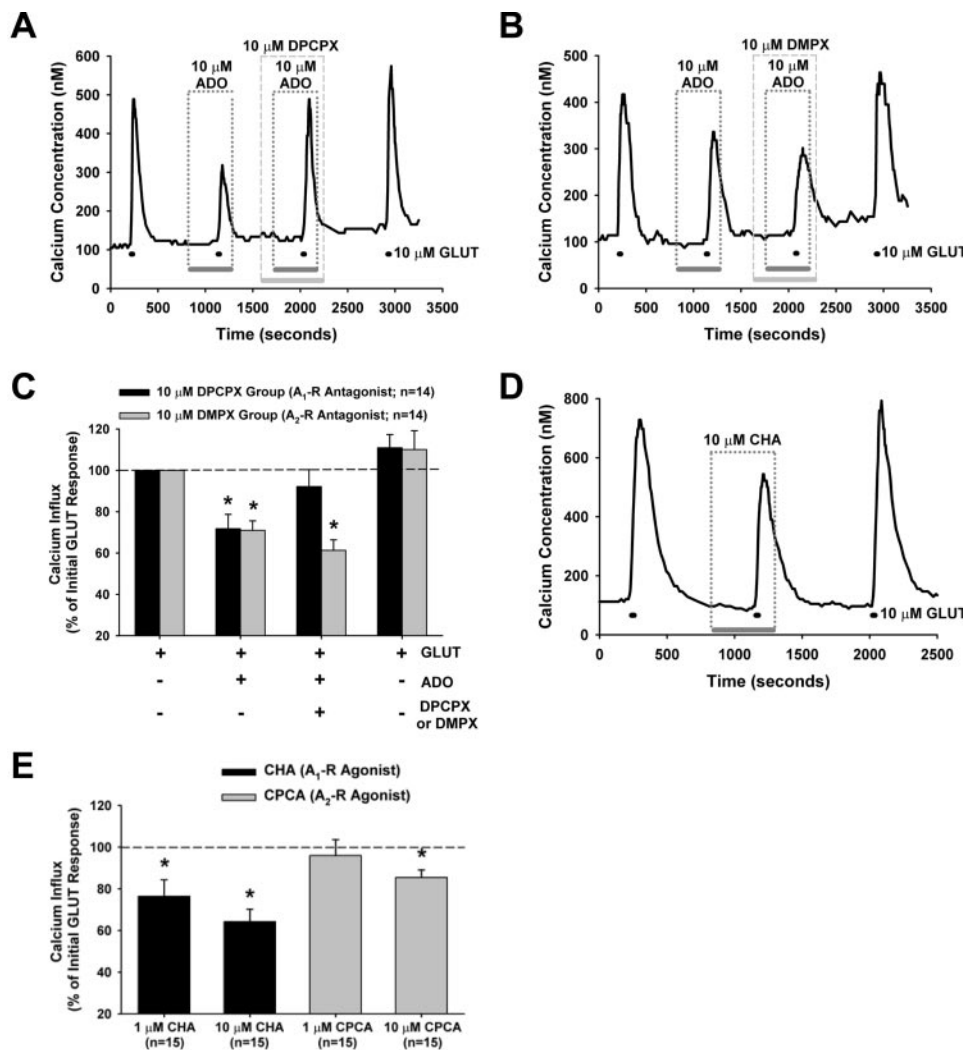


**FIGURE 3.** Effect of A<sub>1</sub>-R and A<sub>2</sub>-R antagonists and agonists on glutamate-induced calcium influx in isolated RGCs.  $[Ca^{2+}]_i$  traces from individual RGCs showing (A) the A<sub>1</sub>-R antagonist DPCPX (10  $\mu$ M) nearly completely blocked the inhibitory effect of 10  $\mu$ M adenosine (ADO) on increases in  $[Ca^{2+}]_i$  induced by 10  $\mu$ M glutamate (GLUT; with 10  $\mu$ M glycine), whereas (B) the A<sub>2</sub>-R antagonist DMPX (10  $\mu$ M) had little effect. (C) Mean data for studies with adenosine receptor antagonists, normalized to initial response (dashed line, 100%). (D) Trace illustrating effect of the A<sub>1</sub>-R agonist CHA. (E) Mean data for studies with the A<sub>1</sub>-R agonist CHA (1 or 10  $\mu$ M) or the A<sub>2</sub>-R agonist CPCA (1 or 10  $\mu$ M), normalized to the initial response (dashed line, 100%). \* $P < 0.01$  compared with both the initial and recovery responses to glutamate (Friedman ANOVA, SNK).

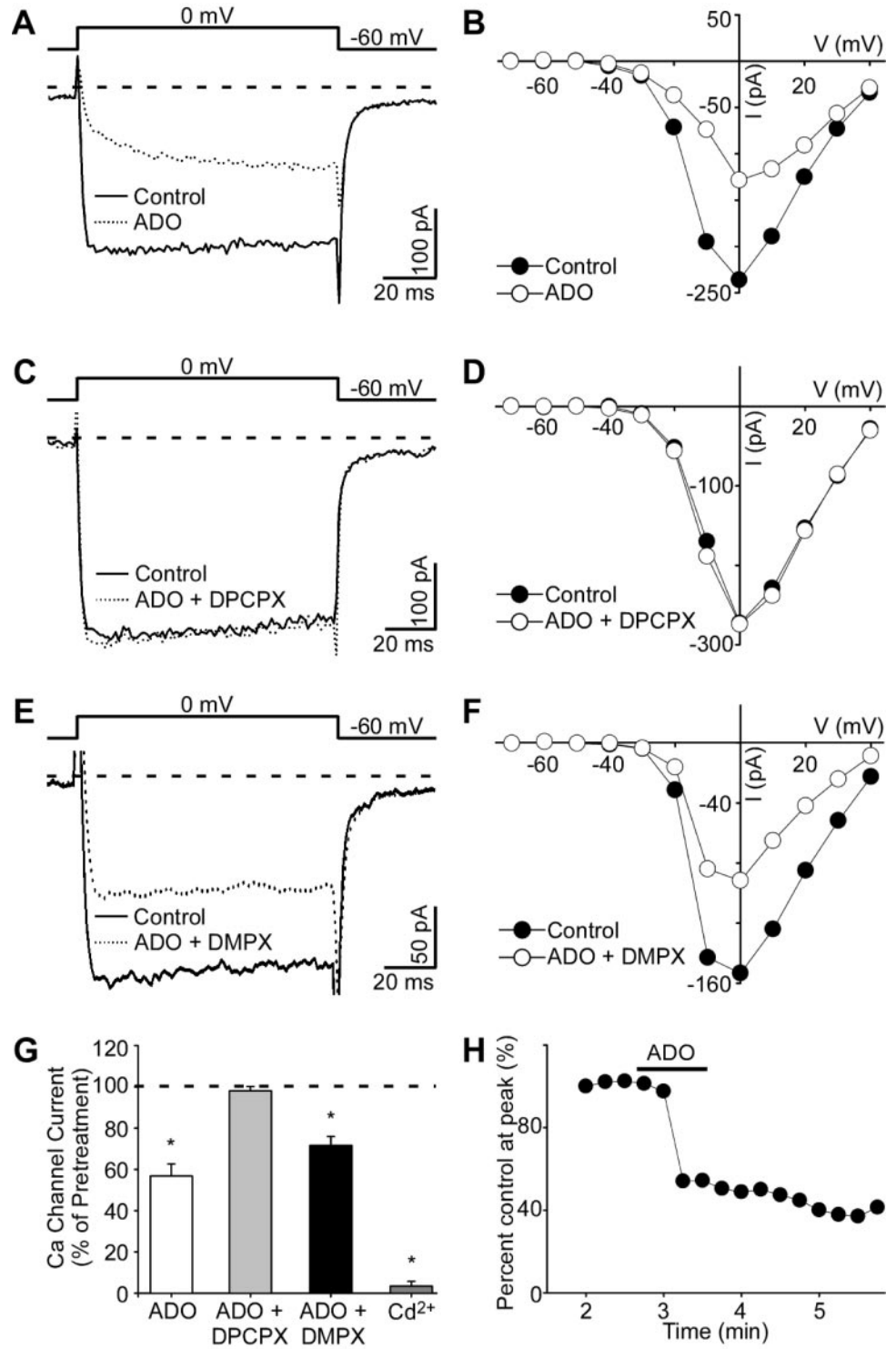


**FIGURE 4.** Adenosine (ADO) inhibited VGCC currents in isolated RGCs through A<sub>1</sub>-Rs. (A) Current traces to a 0-mV step and (B) I-V relations of the same isolated RGC in control conditions and in the presence of 10 μM adenosine, showing the decrease in calcium channel currents with adenosine. (C) Current traces and (D) I-V relation in an isolated RGC, showing that 10 μM adenosine did not affect calcium channel currents when the A<sub>1</sub>-R antagonist DPCPX (10 μM) was present. (E) Current traces and (F) I-V relations showing that 10 μM adenosine decreased calcium channel currents when the A<sub>2</sub>-R antagonist DMPX (10 μM) was present. (G) Data summary for the effects of 10 μM adenosine alone (*n* = 7) and in combination with DPCPX (10 μM; *n* = 5) or DMPX (10 μM; *n* = 5), and the effect of the nonspecific VGCC blocker cadmium (Cd<sup>2+</sup>; 100 μM; *n* = 8) on calcium channel currents at 0 mV. \**P* < 0.01 compared with current before drug treatment (Mann-Whitney). (H) Time course of fast adenosine action illustrating its fast inhibitory effect on the current.

the presence of the A<sub>1</sub>-R antagonist DPCPX, the inhibitory effect of adenosine was blocked, and the current was not significantly different (mean inhibition, 1.9% ± 2.1%; *n* = 5; *P* = 0.69) from the current before drug treatment (Figs. 4C, 4D, 4G). In contrast, in the presence of the A<sub>2</sub>-R antagonist DMPX, adenosine still significantly inhibited (mean inhibition, 28.4% ± 4.3%; *n* = 5; *P* < 0.01) the calcium channel current (Figs. 4E, 4F, 4G). The current was completely blocked by 100 μM cadmium (mean inhibition, 96.5% ± 2.4%; *n* = 8), indicating that this current was mediated by VGCCs (Fig. 4G). The time course of the inhibition by adenosine on calcium channel currents was fast, and under the recording conditions used in

the electrophysiology experiments (e.g., ruptured patch whole-cell recording), the effect of adenosine was generally not reversible (Fig. 4H).

**Effect of Adenosine on NMDA-Induced Calcium Influx in RGCs in Retinal Wholemounts**

Injection of fura dextran into flatmounted rat retina resulted in the loading of the dye into RGC axons that passed through the injection site, and, after 3 to 5 hours, the dye was retrogradely transported to RGC somata. In this study, all experiments were performed on retrogradely labeled cells that were at least 200

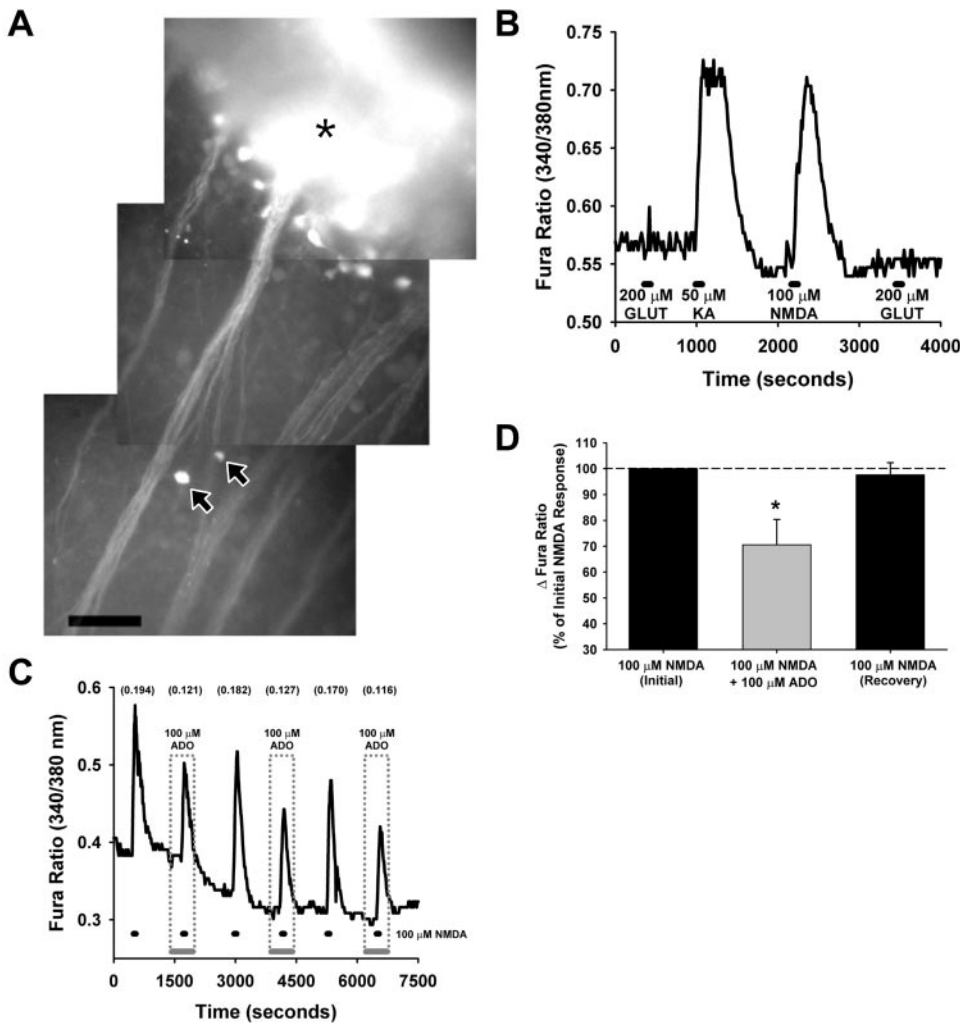


**FIGURE 5.** Adenosine (ADO) inhibited NMDA-induced calcium influx in RGCs in rat retinal wholemounts. **(A)** Montage of fluorescence micrographs showing two RGCs (*arrows*) retrogradely loaded with the fura dextran calcium indicator dye, located in the vicinity of labeled axon bundles. The fura dextran had been injected  $\sim 3$  hours earlier at the site denoted with an *asterisk*. Scale bar,  $50 \mu\text{m}$ . **(B)** Representative trace from an RGC illustrating that the glutamate agonists NMDA and kainate (KA), but not glutamate (GLUT), induced increases in  $[\text{Ca}^{2+}]_i$  in the intact retina. **(C)** Trace illustrating the effect of adenosine on NMDA-induced calcium influx in an RGC in the intact retina. The cell was exposed to NMDA six times with adenosine present during the second, fourth, and sixth treatments. The numbers in parentheses are the  $\Delta$ fura ratios (peak ratio minus baseline ratio) for each response. **(D)** Summary of data for the effect of adenosine on RGCs ( $n = 5$ ) in the intact retina preparations, normalized to initial NMDA response (*dashed line*).  $*P < 0.05$  compared with both initial and recovery NMDA responses (Friedman ANOVA, SNK).

$\mu\text{M}$  from the injection site and that were located in the GCL near bundles of labeled axons (Fig. 5A). Although there are displaced amacrine cells in the rat GCL, it is rare for these cells to have a dendritic spread larger than  $200 \mu\text{m}$ .<sup>22</sup> Thus, it is highly likely that the cells used for these experiments were RGCs and not displaced amacrine cells.

Exogenous application of  $200 \mu\text{M}$  glutamate had no effect on RGC calcium levels in the flatmounted rat retinas (Fig. 5B) due to the presence of functional high-affinity glutamate uptake systems, consistent with previous electrophysiological studies using intact retina preparations.<sup>23</sup> In contrast, the glutamate agonists NMDA and kainate, which are not recognized by the neuronal and glial glutamate transporters, consistently elevated RGC  $[\text{Ca}^{2+}]_i$  (Fig. 5B). Thus,  $100 \mu\text{M}$  NMDA was used to elevate  $[\text{Ca}^{2+}]_i$  in the experiments on the flatmounted retinas.

Adenosine ( $100 \mu\text{M}$ ) significantly decreased ( $P < 0.05$ ) the NMDA-induced calcium influx in the RGCs ( $n = 5$ ; cells from five different retinas from four rats) in the intact rat retina preparation (Figs. 5C, 5D). The mean change in the fura ratio (peak ratio minus baseline ratio) in the presence of adenosine was  $70.5 \pm 9.8\%$  of that in the initial response to NMDA alone. In the third exposure to NMDA after adenosine treatment, the RGCs exhibited recovery in which the mean response was  $97.6 \pm 4.8\%$  of the initial response. In the optical recording shown in Figure 5C, the tested cell was exposed to NMDA six times, alternating between the presence and absence of adenosine, which illustrates that the effect of adenosine was reversible and repeatable (the first three responses in

this cell were used for the analysis shown in Fig. 5D). The gradual decrease in baseline (Fig. 5C) was sometimes observed in the intact retina experiments and was probably due to the changing background fluorescence, as fura dextran on the retinal surface (excess spillage from the injection) was washed away during the experiment. By quantifying calcium influx as the change in fura ratio (calculated as the peak minus baseline ratio) for each response in these experiments on the intact retina, this artifact did not influence the results.

## DISCUSSION

In this study, adenosine decreased glutamate-induced calcium influx and VGCC currents in isolated neonatal mammalian (rat) retinal ganglion cells obtained from purified cultures produced by immunopanning. Adenosine also decreased NMDA-induced calcium influx in adult rat RGCs in an intact retina preparation, confirming that the effects of adenosine on RGCs are not unique to neonates or due to an artifact produced by the *in vitro* preparation.

In agreement with previous reports,<sup>14,15</sup> the immunopanning method generated highly purified RGC cultures. After the retrograde labeling of RGCs, by application of rhodamine dextran to the superior colliculus in preliminary experiments, more than 97% of the panned cells contained the label. The small percentage ( $< 3\%$ ) of unlabeled cells could be RGCs that were not retrogradely labeled or could represent other retinal neurons that escaped removal during the final rinse of the

Thy1.1 panning plate. We think the latter is most likely, given that the unlabeled cells were generally smaller and morphologically distinct from labeled RGCs. Cells of this type were not used for the calcium imaging or electrophysiology experiments.

Glutamate is the principal neurotransmitter of the retina and mediates synaptic communication between bipolar cells and RGCs. Therefore, to assess potential postsynaptic modulation of excitatory input to RGCs, glutamate was used to stimulate calcium influx in the cultured RGCs. Glutamate could increase  $[Ca^{2+}]_i$  directly, by activating NMDA receptor-gated channels, or indirectly by activation of VGCCs after RGC depolarization due to stimulation of NMDA and non-NMDA glutamate receptors.<sup>24</sup> To stimulate both pathways, we used conditions that would promote NMDA receptor activation. Specifically, extracellular  $Mg^{2+}$  was removed during calcium-imaging experiments, to eliminate the voltage-dependent block by this cation of NMDA receptors,<sup>25,26</sup> and glycine, a known coagonist of glutamate at NMDA receptors,<sup>18</sup> was added to the glutamate solution.

Based on receptor binding studies in the rat brain, DPCPX and DMPX have been shown to be selective adenosine receptor antagonists (relative affinity ratio  $[A_2K_i/A_1K_i] = 739$  for DPCPX and 0.35 for DMPX).<sup>27</sup> The inhibitory effect of adenosine on glutamate-induced calcium influx was blocked by the  $A_1$ -R antagonist DPCPX, whereas the  $A_2$ -R antagonist DMPX had little effect, demonstrating an  $A_1$ -R-mediated mechanism. In addition, the selective  $A_1$ -R agonist CHA (1 and 10  $\mu M$ ) was more effective than the  $A_2$ -R agonist CPCA (1 and 10  $\mu M$ ) at reducing glutamate-dependent increases of RGC  $[Ca^{2+}]_i$ . At 10  $\mu M$  CPCA had a small but significant effect, but this is probably due to an action at  $A_1$ -Rs, as CPCA is not completely selective for the  $A_2$ -R (relative affinity ratio  $[A_2K_i/A_1K_i] = 392$  for CHA and 2.1 for CPCA; from binding studies in rat brain).<sup>28</sup> The pharmacological characterization in this study of functional  $A_1$ -Rs on RGCs is consistent with prior anatomic studies that have identified the presence of these receptors in the GCL.<sup>6-8</sup>

Despite the benefits associated with the use of the purified RGC cultures, it could be argued that the dissociation and panning procedure, performed on neonatal retinas, generates RGCs with different characteristics than those in the adult retina with retinal synaptic connections intact. Our finding that adenosine inhibited NMDA-induced calcium influx in RGCs in flatmounted retinal preparations indicates that the neuromodulatory action of adenosine was not unique to the isolated RGCs. A possible disadvantage with the intact retina preparation is that there is the potential for adenosine to act upstream from RGCs in the retinal visual pathway. For example, it has been shown recently in salamanders that adenosine, through  $A_2$ -R activation, can inhibit glutamate release from rod photoreceptors.<sup>29,30</sup> However, NMDA receptors have been localized primarily to RGCs, and some amacrine cells in the mammalian retina,<sup>23</sup> and so it is unlikely that the decrease in NMDA-induced RGC  $[Ca^{2+}]_i$  by adenosine observed in the present study was an indirect effect due to an inhibition of glutamate release from photoreceptors or bipolar cells. Taken together with the results from the cultured RGCs, this work provides strong evidence that adenosine modulates the glutamatergic input to mammalian RGCs. The method of retrogradely loading RGC somata with dextran-conjugated calcium indicator dye was originally developed in the rabbit retina,<sup>21</sup> and the present study shows that this technique can be applied to the rat retina as well.

The best established action of  $A_1$ -Rs in the CNS is presynaptic inhibition of neurotransmitter release due to modulation of VGCCs (predominantly N-type) in neuronal terminals.<sup>31-34</sup> Indeed,  $A_1$ -R-mediated inhibition of presynaptic neurotransmitter release has been demonstrated at RGC axon terminals, which are located in the brain.<sup>9,10,12</sup> However, the potential

colocalization of adenosine and  $A_1$ -Rs in the inner retina<sup>6-8</sup> implies that adenosine may exert postsynaptic modulatory actions on RGCs within the retina itself, and the results from the calcium-imaging experiments in this study indicate that this is possible. It was also shown that adenosine, acting through  $A_1$ -Rs, can decrease calcium currents in rat RGCs, and these results suggest that the observed effect of adenosine on glutamate-induced calcium influx may, at least in part, be attributable to the inhibition of VGCCs. Similar to our findings in RGCs, the postsynaptic modulation of excitatory input by adenosine has been observed in subpopulations of isolated hippocampal<sup>35</sup> and hypothalamic<sup>36</sup> neurons. Further evidence for the role of adenosine in the retina was shown in a recent study, in which adenosine was observed to induce an outward potassium ( $K^+$ ) current in rat RGCs.<sup>37</sup> The  $K^+$  efflux would serve to hyperpolarize the membrane potential, resulting in reduced RGC excitability. Together with the results from the present study, these data make it clear that adenosine can act on mammalian RGCs within the retina, influencing RGCs through the modulation of postsynaptic  $Ca^{2+}$  and  $K^+$  currents and  $[Ca^{2+}]_i$ .

The finding that adenosine can affect glutamate-induced calcium influx in RGCs has potential physiological and pathologic implications. Throughout the CNS,  $A_1$ -R activation is associated with a reduction in neuronal activity and energy expenditure and is thought to contribute to tonic depression of synaptic transmission.<sup>1,33,38</sup> There is evidence, from studies using a perfused feline eye preparation, that there is a tonic level of extracellular adenosine in the retina and that this contributes to an overall inhibition of light-stimulated retinal neuronal activity.<sup>39</sup> The tonic stimulation of RGC  $A_1$ -Rs would dampen the excitatory input to these retinal output neurons and could serve as a fine-tuning mechanism controlling the flow of visual information to the brain. In addition to the role of glutamate in normal synaptic transmission, excessive activation of glutamate receptors can lead to an increase in  $[Ca^{2+}]_i$  to toxic levels, resulting in neuronal death.<sup>40,41</sup> Compounds that limit these increases in  $[Ca^{2+}]_i$  have been shown to protect retinal neurons against glutamate excitotoxicity,<sup>42,43</sup> and thus our results present a mechanism through which adenosine could mediate neuroprotective effects on RGCs. In fact, it is well-established that extracellular adenosine levels increase after ischemia or excitotoxic insults in the CNS, and  $A_1$ -R agonists have exhibited neuroprotective properties in several CNS models of ischemia and excitotoxicity.<sup>1,2,44</sup> In support of the role of adenosine as an endogenous neuroprotective agent, mice lacking  $A_1$ -Rs show impaired functional recovery after ischemia.<sup>38</sup> Increased adenosine levels after ischemia have also been reported in the retina, and there is evidence that the subsequent  $A_1$ -R activation contributes to an endogenous retinal neuroprotective response to limit damage and increase tolerance to future ischemic episodes.<sup>45,46</sup>

In summary, in this study adenosine reduced glutamate-induced calcium influx and inhibited VGCCs in rat RGCs through the activation of  $A_1$ -Rs. This work supports the role of adenosine as a neuromodulator in the mammalian retina, and the postsynaptic effects of adenosine on RGCs could influence physiological and pathologic glutamatergic signaling pathways.

## References

- Dunwiddie TV, Masino SA. The role and regulation of adenosine in the central nervous system. *Annu Rev Neurosci.* 2001;24:31-55.
- Latini S, Pedata F. Adenosine in the central nervous system: release mechanisms and extracellular concentrations. *J Neurochem.* 2001; 79:463-484.
- Neal M, Cunningham J. Modulation by endogenous ATP of the light-evoked release of ACh from retinal cholinergic neurones. *Br J Pharmacol.* 1994;113:1085-1087.

4. Newman EA. Propagation of intercellular calcium waves in retinal astrocytes and Muller cells. *J Neurosci*. 2001;21:2215-2223.
5. Fredholm BB, AP IJ, Jacobson KA, Klotz KN, Linden J. International Union of Pharmacology. XXV. Nomenclature and classification of adenosine receptors. *Pharmacol Rev*. 2001;53:527-552.
6. Blazynski C, Perez MT. Adenosine in vertebrate retina: localization, receptor characterization, and function. *Cell Mol Neurobiol*. 1991;11:463-484.
7. Braas KM, Zarbin MA, Snyder SH. Endogenous adenosine and adenosine receptors localized to ganglion cells of the retina. *Proc Natl Acad Sci USA*. 1987;84:3906-3910.
8. Kvanta A, Seregard S, Sejersen S, Kull B, Fredholm BB. Localization of adenosine receptor messenger RNAs in the rat eye. *Exp Eye Res*. 1997;65:595-602.
9. Zhang C, Schmidt JT. Adenosine A1 and class II metabotropic glutamate receptors mediate shared presynaptic inhibition of retinotectal transmission. *J Neurophysiol*. 1999;82:2947-2955.
10. Zhang C, Schmidt JT. Adenosine A1 receptors mediate retinotectal presynaptic inhibition: uncoupling by C-kinase and role in LTP during regeneration. *J Neurophysiol*. 1998;79:501-510.
11. Sun X, Barnes S, Baldrige WH. Adenosine inhibits calcium channel currents via A1 receptors on salamander retinal ganglion cells in a mini-slice preparation. *J Neurochem*. 2002;81:550-556.
12. Hallworth R, Cato M, Colbert C, Rea MA. Presynaptic adenosine A1 receptors regulate retinohypothalamic neurotransmission in the hamster suprachiasmatic nucleus. *J Neurobiol*. 2002;52:230-240.
13. Brewer GJ. Isolation and culture of adult rat hippocampal neurons. *J Neurosci Methods*. 1997;71:143-155.
14. Barres BA, Silverstein BE, Corey DP, Chun LL. Immunological, morphological, and electrophysiological variation among retinal ganglion cells purified by panning. *Neuron*. 1988;1:791-803.
15. Meyer-Franke A, Kaplan MR, Pfrieger FW, Barres BA. Characterization of the signaling interactions that promote the survival and growth of developing retinal ganglion cells in culture. *Neuron*. 1995;15:805-819.
16. Brewer GJ, Torricelli JR, Evege EK, Price PJ. Optimized survival of hippocampal neurons in B27-supplemented Neurobasal, a new serum-free medium combination. *J Neurosci Res*. 1993;35:567-576.
17. Potts RA, Dreher B, Bennett MR. The loss of ganglion cells in the developing retina of the rat. *Brain Res*. 1982;255:481-486.
18. Johnson JW, Ascher P. Glycine potentiates the NMDA response in cultured mouse brain neurons. *Nature*. 1987;325:529-531.
19. Grynkiewicz G, Poenie M, Tsien RY. A new generation of Ca<sup>2+</sup> indicators with greatly improved fluorescence properties. *J Biol Chem*. 1985;260:3440-3450.
20. Kao JP. Practical aspects of measuring [Ca<sup>2+</sup>] with fluorescent indicators. *Methods Cell Biol*. 1994;40:155-181.
21. Baldrige WH. Optical recordings of the effects of cholinergic ligands on neurons in the ganglion cell layer of mammalian retina. *J Neurosci*. 1996;16:5060-5072.
22. Perry VH. The ganglion cell layer of the retina of the rat: a Golgi study. *Proc R Soc Lond B Biol Sci*. 1979;204:363-375.
23. Thoreson WB, Witkovsky P. Glutamate receptors and circuits in the vertebrate retina. *Prog Retin Eye Res*. 1999;18:765-810.
24. Berridge MJ. Neuronal calcium signaling. *Neuron*. 1998;21:13-26.
25. Nowak L, Bregestovskij P, Ascher P, Herbert A, Prochiantz A. Magnesium gates glutamate-activated channels in mouse central neurones. *Nature*. 1984;307:462-465.
26. Mayer ML, Westbrook GL, Guthrie PB. Voltage-dependent block by Mg<sup>2+</sup> of NMDA responses in spinal cord neurones. *Nature*. 1984;309:261-263.
27. Jacobson KA, Van Rhee AM. Development of selective purinoceptor agonists and antagonists. In: Jacobson KA, Jarvis MF, eds. *Purinergic Approaches in Experimental Therapeutics*. New York: Wiley-Liss; 1997.
28. Bruns RF, Lu GH, Pugsley TA. Characterization of the A2 adenosine receptor labeled by [3H]NECA in rat striatal membranes. *Mol Pharmacol*. 1986;29:331-346.
29. Stella SL Jr, Bryson EJ, Thoreson WB. A2 adenosine receptors inhibit calcium influx through L-type calcium channels in rod photoreceptors of the salamander retina. *J Neurophysiol*. 2002;87:351-360.
30. Stella SL Jr, Bryson EJ, Cadetti L, Thoreson WB. Endogenous adenosine reduces glutamatergic output from rods through activation of A2-like adenosine receptors. *J Neurophysiol*. 2003;90:165-174.
31. Yawo H, Chuhma N. Preferential inhibition of omega-cenotoxin-insensitive presynaptic Ca<sup>2+</sup> channels by adenosine autoreceptors. *Nature*. 1993;365:256-258.
32. Mogul DJ, Adams ME, Fox AP. Differential activation of adenosine receptors decreases N-type but potentiates P-type Ca<sup>2+</sup> current in hippocampal CA3 neurons. *Neuron*. 1993;10:327-334.
33. Wu LG, Saggau P. Adenosine inhibits evoked synaptic transmission primarily by reducing presynaptic calcium influx in area CA1 of hippocampus. *Neuron*. 1994;12:1139-1148.
34. Scammell TE, Arrigoni E, Thompson MA, Ronan PJ, Saper CB, Greene RW. Focal deletion of the adenosine A1 receptor in adult mice using an adeno-associated viral vector. *J Neurosci*. 2003;23:5762-5770.
35. de Mendonca A, Sebastiao AM, Ribeiro JA. Inhibition of NMDA receptor-mediated currents in isolated rat hippocampal neurones by adenosine A1 receptor activation. *Neuroreport*. 1995;6:1097-1100.
36. Obrietan K, Belousov AB, Heller HC, van den Pol AN. Adenosine pre- and postsynaptic modulation of glutamate-dependent calcium activity in hypothalamic neurons. *J Neurophysiol*. 1995;74:2150-2162.
37. Newman EA. Glial cell inhibition of neurons by release of ATP. *J Neurosci*. 2003;23:1659-1666.
38. Johansson B, Halldner L, Dunwiddie TV, et al. Hyperalgesia, anxiety, and decreased hypoxic neuroprotection in mice lacking the adenosine A1 receptor. *Proc Natl Acad Sci USA*. 2001;98:9407-9412.
39. Kaelin-Lang A, Jurklics B, Niemeyer G. Effects of adenosinergic agents on the vascular resistance and on the optic nerve response in the perfused cat eye. *Vision Res*. 1999;39:1059-1068.
40. Choi DW. Glutamate neurotoxicity and diseases of the nervous system. *Neuron*. 1988;1:623-634.
41. Leist M, Nicotera P. Apoptosis, excitotoxicity, and neuropathology. *Exp Cell Res*. 1998;239:183-201.
42. Baptiste DC, Hartwick AT, Jollimore CA, et al. Comparison of the neuroprotective effects of adrenoceptor drugs in retinal cell culture and intact retina. *Invest Ophthalmol Vis Sci*. 2002;43:2666-2676.
43. Kawasaki A, Han MH, Wei JY, Hirata K, Otori Y, Barnstable CJ. Protective effect of arachidonic acid on glutamate neurotoxicity in rat retinal ganglion cells. *Invest Ophthalmol Vis Sci*. 2002;43:1835-1842.
44. de Mendonca A, Sebastiao AM, Ribeiro JA. Adenosine: does it have a neuroprotective role after all? *Brain Res Brain Res Rev*. 2000;33:258-274.
45. Ghiardi GJ, Gidday JM, Roth S. The purine nucleoside adenosine in retinal ischemia-reperfusion injury. *Vision Res*. 1999;39:2519-2535.
46. Li B, Roth S. Retinal ischemic preconditioning in the rat: requirement for adenosine and repetitive induction. *Invest Ophthalmol Vis Sci*. 1999;40:1200-1216.